ACS OMEGA

http://pubs.acs.org/journal/acsodf

Article

Visual Filling Model Experiment Study on the Enhanced Oil Recovery Mechanism of Novel Polymer Viscosity Reducer Flooding in Heavy Oil Reservoirs

Yu Li, Huiqing Liu, Qing Wang,* Xiaohu Dong, and Xin Chen

Cite This: *ACS Omega* 2021, 6, 24663−24671

Read Online

ACCESS | Metrics & More | Article Recommendations

ABSTRACT: Chemical flooding is an effective method to enhance heavy oil recovery, and the viscosity reducer is often injected into the formation as the main reagent of chemical flooding. In the paper, a novel polymer viscosity reducer (FMP) was used to inject into a visual filling model, which can simulate the reservoir. The mechanism of enhancing heavy oil recovery by FMP is studied by macroscopic and microscopic analysis methods. The model can obtain macroscopic images and production data, including pressure, water cut, and oil recovery. The model can observe some microscopic processes, which can analyze the mechanism of enhanced oil recovery. Five processes of emulsifying viscosity reduction are summarized by using microscopic images: membrane oil removal, gradual emulsification, flocculation into droplet groups, active dispersion, and agglomeration into droplets. The FMP molecules can affect the interfacial properties of oil, water, and rock to enhance the wishing oil efficiency. Moreover, the decrease in the stability of the oil−water interface leads to flocculation into droplet groups and agglomeration into droplets occurring at the throat of the strong seepage zone, which increases the sweep coefficient from 0.56 to 0.90. The oil recovery has increased from 18 to 34%, which indicates that the FMP flooding obviously enhances the effect of heavy oil reservoir development.

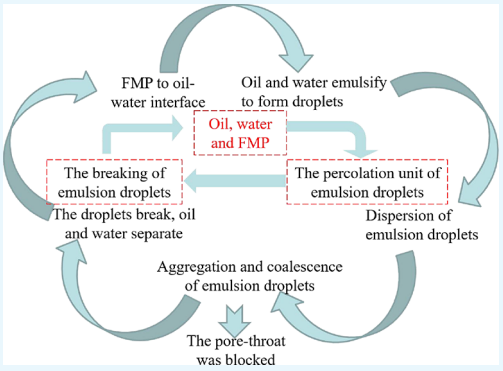

1. INTRODUCTION

Heavy oil is widely distributed in the world and plays an important role in petroleum exploration and development.[1,2] According to previous research, water flooding is difficult to effectively develop with heavy oil with high viscosity. The development technology of heavy oil has still been dominated by steam and thermal exploitation.[3−5] Thus, an efficient and convenient way to reduce the viscosity of heavy oil has become an inevitable choice for oil development.[6−8] Chemical flooding is an important method, which is aimed at improving the fluidity of heavy oil and reducing the percolation resistance in the formation.[9,10] The blockage of emulsion in the pore-throat can promote the reservoir pressure change spread to the unswept area, which is beneficial to developing the heavy oil reservoir.[11]

Many experts and scholars have also proposed some measures for heavy oil development. Huang et al.[12] enhanced oil recovery in glutenite heavy oil reservoirs by gas flooding. Yu et al.[13] studied the effect of surfactant-polymer flooding on the oil recovery in heavy oil reservoirs. Shan et al.[14] used a gel to enhance heavy oil by controlling the profile. Through literature investigation, a polymer surfactant or surfactant-polymer plays a favorable role in enhancing heavy oil recovery.

It is important for enhancing oil recovery to directly reflect the percolation rule by using experimental equipment. Roosta et al.[15] used the glass micromodels to investigate the effect of steam and hot water injection on their wettability. Herbas et al.[16] used the comprehensive micromodel to evaluate polymer enhanced oil recovery (EOR) in unconsolidated sand reservoirs. Zhang et al.[17] introduced multiscale visual models to unravel flow and transport physics in porous media. Pratama et al.[18] used the visual micromodel to find that the phase distribution and wettability state are sensitive to steam phase. With the development of visualization technology, the observation of the development process of simulated reservoirs is strengthened.

In the paper, a novel visual filling model filled with rock particles and cement is used to conduct water flooding and viscosity reducer flooding experiments.[19] The dynamic production data and microscopic percolation images are obtained from the displacement experiments so as to study the mechanism of the novel viscosity reducer flooding to enhance oil recovery.

Received: June 28, 2021
Published: September 13, 2021

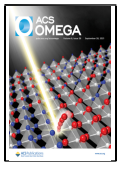

2. EXPERIMENTAL PROCESS

2.1. Materials. The dehydrated and degassed crude oil and formation water were provided by SINOPEC Exploration and Development Research Institute. A multifunctional rheometer (Anton Paar MCR102) was used to measure the viscosity and the density of the oil sample. The viscosity of crude oil at the experimental temperature was 1413.5 MPa·s (Figure 1). The density of the oil was measured as 952 kg/m^3 at 25 °C.

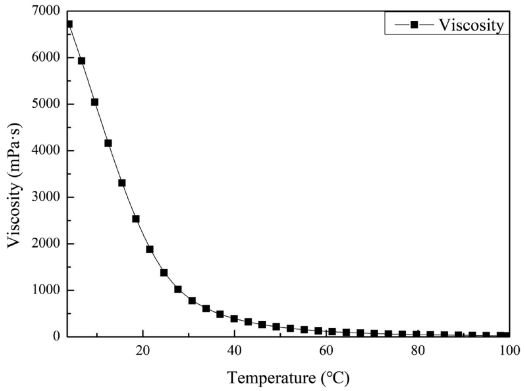

Figure 1. Viscosity−temperature curve of heavy oil.

The salinity of the formation water was measured as 2.86 × 10^4 mg/L. The mineral composition of the formation water used in the experiment is shown in Table 1. The composition of crude oil used in the experiment is shown in Table 2. Formation water was the injected fluid in the water injection phase of the experiment, and it was also the solvent for preparing chemical agent solution.

In the experiment, the novel viscosity reducer is a polymer active viscosity reducer, which is called FMP developed by Sinopec. As shown in Figure 2, the molecular structure of FMP, including AM, AA, PB, and AMPS, can be observed. AM and AA fragments have an effect of increasing the viscosity of the water phase, which plays an important role in the thickening of the water phase and enhances the solubility of FMP molecules. The PB fragment plays an efficient role in the separation of asphaltene. The AMPS fragment has an effect of enhancing interfacial activity, which means that FMP can reduce oil−water interfacial tension.

2.2. Testing of FMP Performance. It is important to study the performance of FMP at different concentrations. At a shear rate of 10.2 s^{-1}, the mixed solution was obtained by mixing the oil−formation water in a ratio of 7:3. A rotary viscometer (NDJ-8S) was used to measure the viscosity of the mixed solution, and the viscosity reduction ratio was calculated:[20]

$$R_o = \frac{\mu_i - \mu_r}{\mu_i} \times 100\% \quad (1)$$

where R_o is the viscosity reduction ratio, μ_i is the apparent viscosity of the oil sample, and μ_r is the apparent viscosity of the oil sample mixed with FMP solution.

The FMP molecules in the solution aggregated toward the oil−water interface due to the low interfacial energy at the oil−water interface, which forms emulsion droplets.[21,22] Because low interfacial tension tends to promote the formation of large numbers of emulsion droplets, it is necessary to test the influence of the FMP solution concentration on the interfacial tension of droplets. A rotating drop surface tensiometer (TX-500C) was used to measure the interfacial tension data of the emulsion droplets.

Under the influence of different FMP solution concentrations, the size of emulsion droplets is obviously different.[23,24] In the paper, it is necessary to test the effect of the FMP solution concentration on the size of emulsion droplets. A Malvern Zetasizer Nano was used to measure the size of emulsion droplets.

2.3. Displacement Experimental Setup. The experimental apparatus consisted of five parts: (1) visual filling model, (2) image acquisition system, (3) pressure acquisition system, (4) fluid injection system, and (5) fluid metering system. As shown in Figure 3, the experimental system was assembled to realize the visual displacement experiment. In particular, it is necessary to place the visual filling model and the fluid injection system in the incubator to control the experimental temperature.

In the paper, we used a novel visual filling model, which was convenient for FMP flooding to obtain macroscopic and microscopic phenomena. There were quartz glass beads that simulated the rock skeleton and thermal-resistant organic glue, which simulated the cement that existed in the space between the two glass plates. The thermal-resistant organic glue and quartz glass beads together formed the simulated reservoir. The simulated reservoir was sealed around with heat-resistant glass glue. The four sides and corners of the model were reinforced with perforated screws, which made quartz glass beads inside the reservoir fit tightly together. Four perforation holes were symmetrically drilled at the four corners of the upper glass panel to simulate four vertical wells. The model had a porosity of 0.35 and a permeability of 1.89 Darcy after the physical tests.

The image acquisition system used a digital camera and Sweden Optilia optical microscope, which could transmit macroscopic and microscopic images to the computer. Pressure sensors and electronic balances transmitted pressure and production data to the computer through the automated data acquisition.

The procedure of the displacement experiment is as follows: (1) The air tightness of the experimental apparatus was checked. (2) The ISCO pump flow rate was 0.3 mL /min to inject oil into the visual filling model. (3) The model was placed at the experimental temperature and stood for more than 72 h. (4) The flow rate of the ISCO pump was set at 0.5 mL/min to inject formation water into the model to simulate water flooding. (5) When the water cut reached 98%, the ISCO pump started to inject FMP solution into the model to simulate FMP flooding. (6) When the water cut reached 98% again, the ISCO pump was shut down to stop displacement.

Table 2. Composition of Crude Oil (25 °C)

saturated hydrocarbon (%)	aromatic hydrocarbon (%)	resin (%)	asphaltene (%)
15.6	28.2	42.8	13.4

Table 1. Ion Content and Salinity of Formation Water

ion content	Na^+	Mg^{2+}	Ca^{2+}	CO_3^{2-}	HCO_3^-	Cl^-	SO_4^{2-}	total
concentration (mg/L)	9121	152.2	320.2	2726.2	11606.4	4452.6	250.8	28629.4

https://doi.org/10.1021/acsomega.1c03366
ACS Omega 2021, 6, 24663−24671

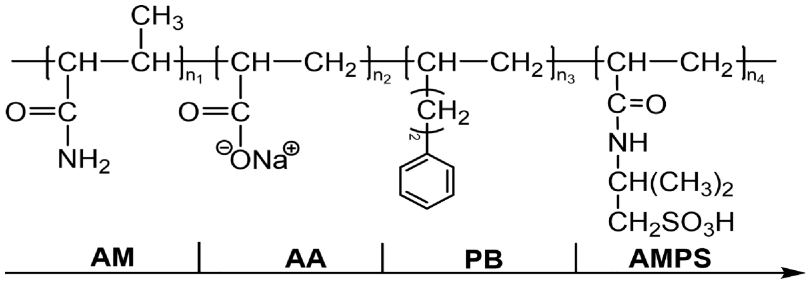

Figure 2. Molecular structure of FMP.

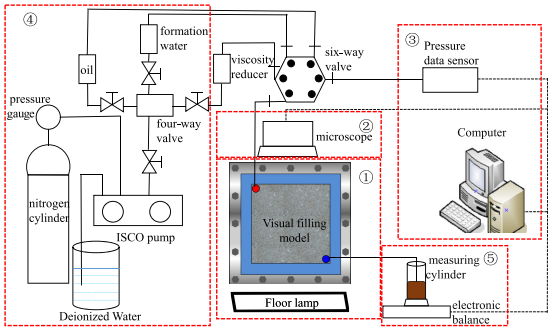

Figure 3. Schematic diagram of the displacement experiment.

3. RESULTS AND DISCUSSION

3.1. Evaluation of FMP Performance. Different concentrations of FMP solutions were mixed with crude oil to make mixed solutions. As shown in Table 3, the viscosity of different concentrations of FMP solutions mixed with oil.

Table 3. Viscosity Reduction Ratio with Different Concentrations of FMP Solutions

concentration of FMP (%)	viscosity (mPa·s)	viscosity reduction ratio (%)
0.2	1067.6	24.4712
0.5	720.2	49.0485
0.8	359.5	80.4386
1	88.7	93.7248
1.2	74.4	94.7365
1.5	67.2	95.2458

The experimental results show that the viscosity reduction ratio is positively correlated with the concentration of FMP solution in a range of 0.2−1.5%. When the concentration of FMP solution exceeds 1%, the increase in the viscosity reduction ratio becomes slow, which indicates that the viscosity reduction effect of the increasing FMP concentration is not obvious under a high FMP concentration. According to the results, FMP solution with a concentration of 1% is selected as the injection solution in the displacement experiment.

The FMP reduces the oil−water interfacial tension, which is beneficial to enhance the percolation ability of the oil phase. It is important to test the oil−water interfacial tension with different FMP concentrations mixed with oil as shown in Table 4.

The results show that it is easy to achieve the lower oil−water interfacial tension under the condition of a lower FMP concentration.

The matching degree of particle size of emulsion droplets and pore-throat size is important for oil migration in the porous media. As shown in Figure 4, FMP concentrations have a great influence on the particle size of emulsion droplets.

Table 4. Interfacial Tension with Different FMP Concentrations Mixed with Oil

concentration of FMP (%)	interfacial tension (mN/m)
0	19.82
0.2	0.4129
0.5	0.3808
0.8	0.3688
1	0.3341

The results show that the high concentration of FMP solution makes the emulsion droplet size smaller and the particle size distribution more concentrated.

3.2. Macroscopic Performance of the Displacement Process. The dynamic variation of the macroscopic displacement process in the simulated reservoir is shown in Figure 5. Figure 5a shows that the visualization area of the model was filled with oil in the initial stage. Figure 5b shows that a viscous fingering phenomenon appeared in the early period of water flooding. Figure 5c shows that water gradually approached the production well from the injection well. As shown in Figure 5d, there were several preferential flooding channels forming the seepage zone between the injection well and the production well at the end of water flooding, which was called the "strong seepage zone" (SSZ).

As shown in Figure 5e, a distinct bifurcation, which was called the "extended seepage zone" (ESZ) occurred on both sides of the SSZ in the early period of FMP flooding. With the injection of FMP solution, the ESZ was gradually extended into the production well. As shown in Figure 5f, the ESZ no longer extended at the end of FMP flooding.

At the end of water flooding, there were still a lot of oil spots in the SSZ. After the FMP solution was injected, oil spots gradually subsided in the SSZ, which indicated that FMP flooding could effectively develop the remaining oil in the SSZ. The disappearance of oil spots in the SSZ and the appearance of the ESZ indicated that the FMP solution entered the unswept area and enlarged the sweep area of the reservoir.

The areal sweep coefficient is used to quantitatively characterize the sweep area of the experiment:

$$S_c = \frac{A_S}{A} \tag{2}$$

where S_c is the areal sweep coefficient, A_S is the sweep area, and A is the visual area of the simulated reservoir.

We calculated that the areal sweep coefficient is 0.56 for water flooding and 0.90 for FMP flooding by the image binarization method. Compared with water flooding, the areal sweep coefficient of FMP flooding was increased by 61%, which

https://doi.org/10.1021/acsomega.1c03366
ACS Omega 2021, 6, 24663−24671

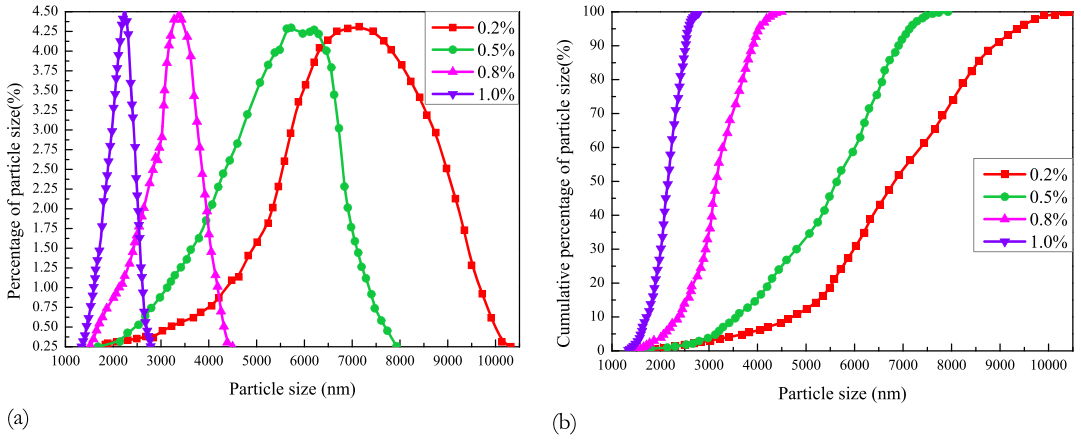

Figure 4. Distribution of emulsion droplets size. (a) Distribution of particle size. (b) Cumulative distribution of particle size.

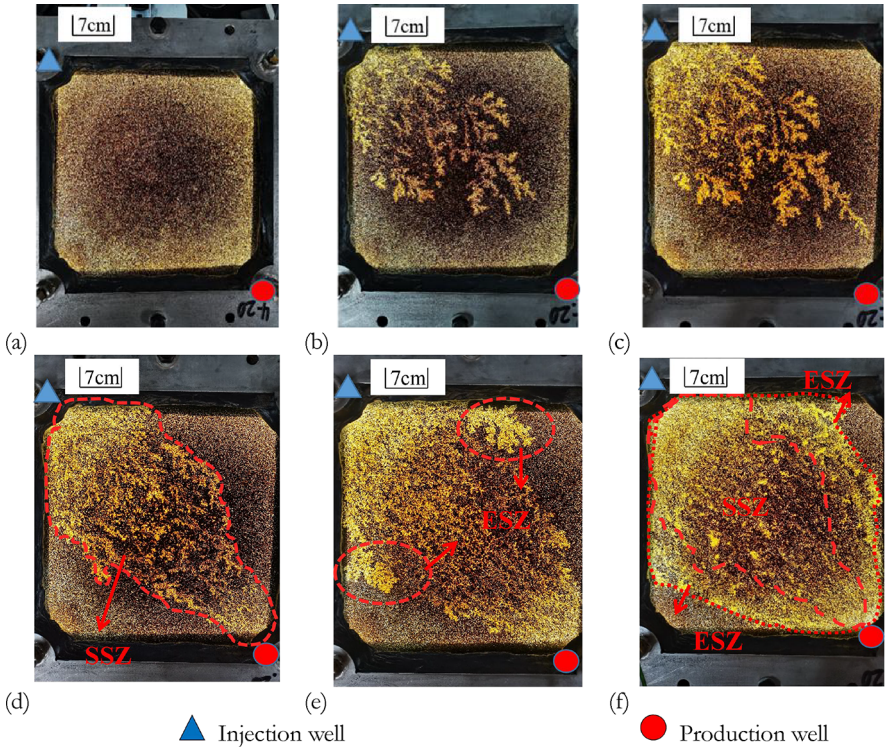

Figure 5. Macroscopic images of the displacement process. (a) Initial state. (b) Fingering phenomenon. (c) Preferential flooding channel. (d) End of water flooding. (e) Appearance of the ESZ. (f) End of the process.

indicated that FMP flooding had an obvious effect on improving the areal sweep coefficient.

Due to the difference in oil−water viscosity in the simulated reservoir, the water flooding front reached the production well quickly. As shown in Figure 6, when the pore volume injection reached 0.5 PV, the water cut exceeded 90%. In the high water cut stage, the injected water mainly flowed in the SSZ, which led to an unobvious increase in oil recovery.

When the FMP flooding began, the pressure gradually increased and the water cut gradually decreased. Compared with the 18% at the end of the water flooding, the oil recovery was increased to 34% at the end of the FMP flooding, which indicated that FMP had a positive effect on the development of the simulated reservoir.

3.3. Microscopic Image of the Displacement Process. After the FMP solution entered the simulated reservoir, a series of changes occurred between FMP and oil−water phases, which played an important role in the development of the simulated reservoir.

3.3.1. Membrane Oil Removal. The process of membrane oil breaking away from the rock surface was called "membrane oil removal", which was the result of the interaction between oil, water, rock, and FMP. After the membrane oil removal, the membrane oil moves into the percolation channel.

The dynamic variation of microscopic images in the membrane oil removal process is shown in Figure 7. Figure 7a shows the initial stage of membrane oil. It could be seen from Figure 7b−d that the connection between the membrane oil and the rock surface became weaker. As time went by, the membrane oil eventually broke away from the rock surface.

When the FMP solution entered the SSZ, FMP molecules spontaneously gathered from the water phase interior to the oil−

https://doi.org/10.1021/acsomega.1c03366
ACS Omega 2021, 6, 24663−24671

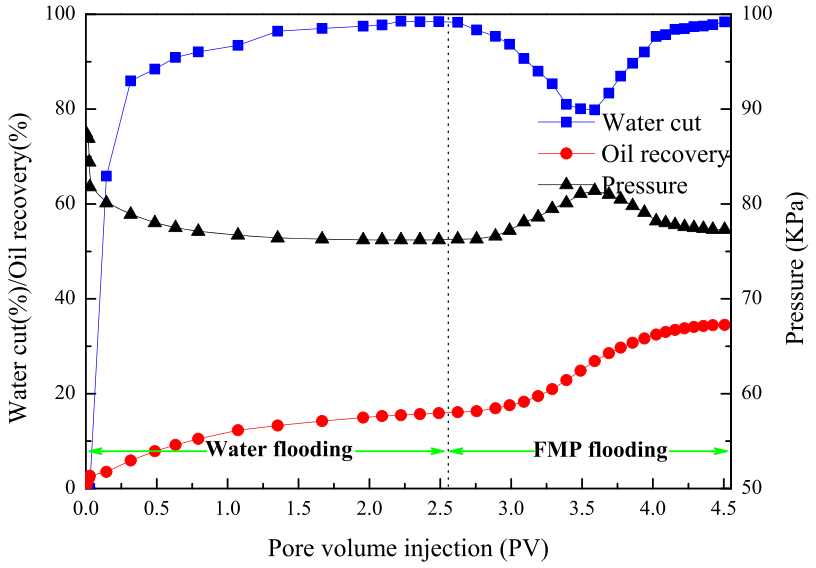

Figure 6. Production dynamic curve of the displacement process.

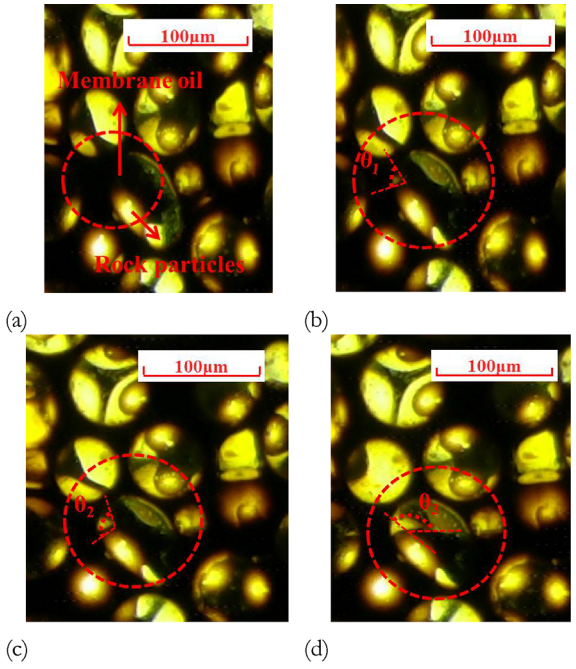

Figure 7. Microscopic image of membrane oil removal. (a) Membrane oil. (b) Deformed membrane oil. (c) Weakening of membrane oil and the rock. (d) Oil and rock to be separated.

water interface whose interfacial energy is low. In particular, when FMP molecules came into contact with the membrane oil, which was adsorbed on the rock surface, FMP molecules affected the wettability of the rock surface.[25,26] As shown in Figure 7, the change of wettability made the connection between the rock surface and the membrane oil gradually became weakened. Moreover, the flow of FMP solution had a tensile effect on the membrane oil, which had weak adsorption ability. Eventually, the membrane oil was removed from the rock surface under the change of wettability and the tensile effect of FMP solution.

Due to the irreversible adsorption of FMP molecules at the rock surface, the FMP molecules would not return to the fluid spontaneously, which resulted in a decrease in the FMP solution concentration.

3.3.2. Gradual Emulsification. After the membrane oil removal stage, the membrane oil, which was removed from the rock surface, enters the moving fluid. The process of the irregular oil droplets to regular emulsion droplet was called "gradual emulsification".

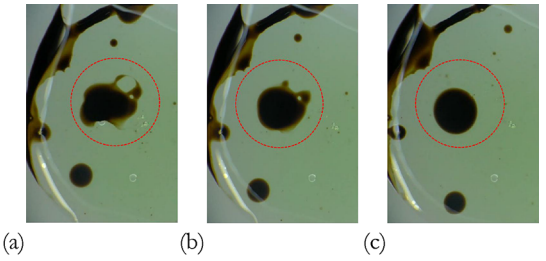

Figure 8. Images of gradual emulsification. (a) Irregular morphology. (b) Contracting oil membrane. (c) Regular droplet shape.

The dynamic variation of microscopic images in the gradual emulsification process is shown in Figure 8. Figure 8a shows the irregular oil droplet. As shown in Figure 8b, the edges of the oil droplet shrunk inward, which caused the droplet to tend to form a regular circle. Eventually, the irregular oil droplet changed into the regular emulsion droplet as shown in Figure 8c. Compared with the irregular oil droplets, the regular emulsion droplets had better mobility, which meant that emulsion droplets were beneficial for the oil to flow through the porous media.

Table 4 shows that the FMP solution had an obvious effect on reducing the oil−water interfacial tension. Because the FMP acted at the oil−water interface resulting in the oil−water interfacial tension decreasing, low interfacial tension causes the emulsion to tend to form the smallest interface, which leads to the irregular membrane oil gradually being transformed to a round emulsion droplet with the smallest interface.

Due to the reversible adsorption of FMP molecules at the oil−water interface, gradual emulsification consumes a small amount of FMP molecules, which leads to a small decrease in the FMP solution concentration.

https://doi.org/10.1021/acsomega.1c03366
ACS Omega 2021, 6, 24663−24671

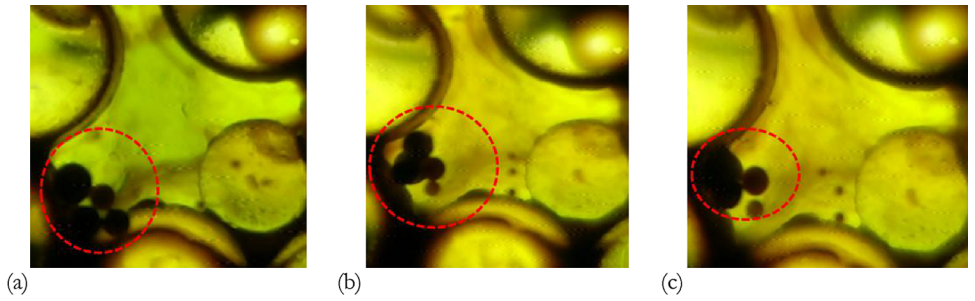

Figure 9. Microscopic image of flocculation into droplet groups. (a) Droplets got close to each other. (b) Droplets bonded to each other. (c) Droplet groups were produced.

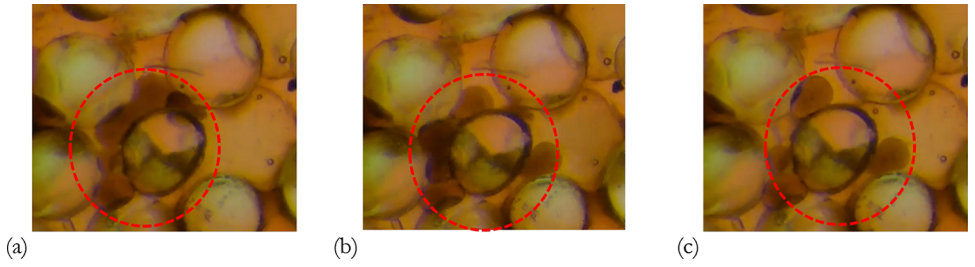

Figure 10. Microscopic image of active dispersion. (a) Droplet groups in the pore throat. (b) Dispersed droplet group. (c) Droplet passing through the pore-throat.

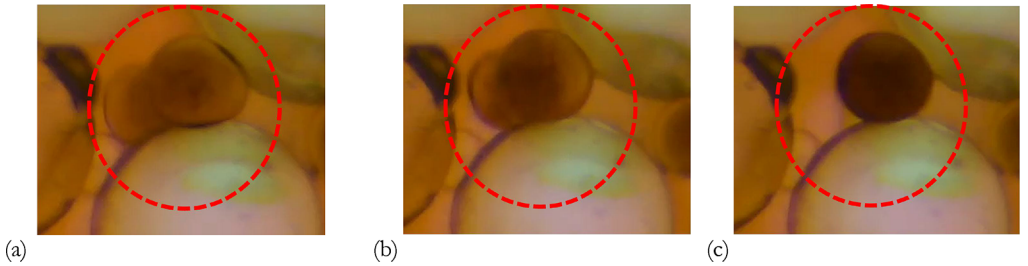

Figure 11. Microscopic image of agglomeration into droplets. (a) Droplet groups near the pore throat. (b) Droplet groups converge. (c) A large emulsion droplet appears.

3.3.3. Flocculation into Droplet Groups. Under the condition of the low FMP concentration and low flow rate, the aggregation process of multiple emulsion droplets in the pores is called "flocculation into droplet groups".

The dynamic variation of microscopic images in the flocculation into droplet group process is shown in Figure 9. As shown in Figure 9a, individual emulsion droplets are close to each other. It can be seen from Figure 9b,c that the water between the droplets was gradually emptied and multiple droplets tended to form droplet groups.

Table 4 shows that the decrease in the FMP concentration led to the increase in interfacial tension, which led to the multiple droplets forming into the droplet group. Many droplets flocculated to form droplet groups, which was adverse to flowing through the pore-throat.[27] Generally speaking, the shape of the droplet groups was related to the shape of the pore-throat.

The multiple emulsion droplets spontaneously flocculated into droplet groups under the conditions of a low concentration and low flow rate, which made the concentration of FMP solution not change.

3.3.4. Active Dispersion. When a high concentration of FMP solution surrounds the droplet groups, the process of restoring the droplet groups with poor mobility to emulsion droplets with better mobility was called "active dispersion".

The dynamic variation of microscopic images in the active dispersion process is shown in Figure 10. As shown in Figure 10a, the shape of the droplet group with poor mobility expands along the shape of the pore throat. It can be seen from Figure 10b,c that the droplet group at the pore-throat gradually disperses into emulsion droplets.

Because the FMP molecules in the fluid flow faster than the droplet groups with poor mobility, the concentration of FMP solution around the droplet groups gradually increases, which makes the interfacial tension of droplet groups decreases again. Under the synergistic effect of fluid shear and FMP concentration increase, FMP molecules are tightly packed at the oil−water interface, which leads to the droplet groups dispersing into several emulsion droplets.[28,29]

Due to the reversible adsorption of FMP molecules at the oil−water interface, active dispersion consumes a small amount of FMP molecules, which leads to a small decrease in the FMP solution concentration.

What is more, flocculation into droplet groups and active dispersion are mutually reversible processes. When the concentration of the FMP solution increases, the droplet groups tend to form emulsion droplets at the "active dispersion" stage. However, when the concentration of FMP solution decreases,

https://doi.org/10.1021/acsomega.1c03366
ACS Omega 2021, 6, 24663−24671

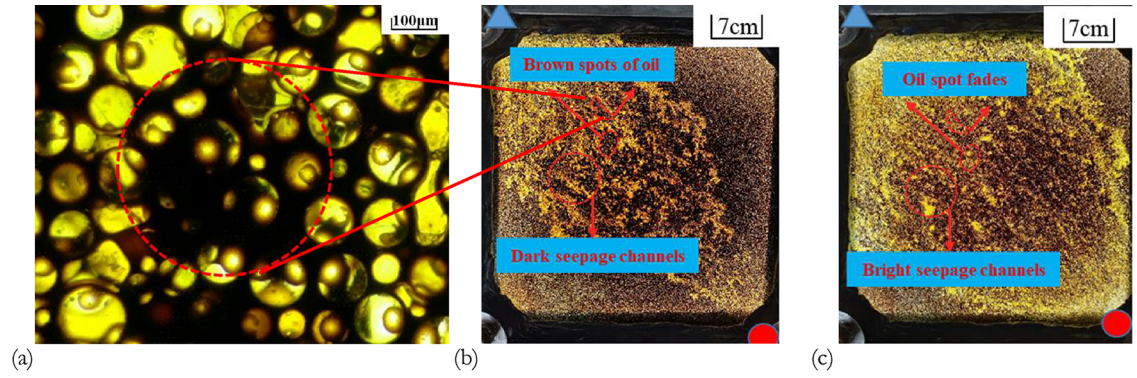

Figure 12. Images of water and FMP flooding. (a) Microscopic image of brown oil spots. (b) Macroscopic image of the water flooding end. (c) Macroscopic image of the FMP flooding end.

the emulsion droplets tend to form droplet groups at the "flocculation into droplet groups" stage.

3.3.5. Agglomeration into Droplets. When the concentration of FMP solution around the droplet groups is low, the process of the droplet group that contracts to form a larger emulsion droplet is called "agglomeration into droplets".

The dynamic variation of microscopic images in the agglomeration into droplet process is shown in Figure 11. As shown in Figure 11a,b, the edges of the droplet group shrunk inward. Eventually, the droplet group changed into a new emulsion droplet as shown in Figure 11c. The volume of the emulsion droplet in Figure 11 did not increase significantly during the process of agglomeration into droplets, but its color deepened significantly. The darker emulsion droplet has a higher percentage of oil in it than the previous emulsion, which indicated that the difference of emulsion droplet and surrounding fluid increased.

The low FMP concentration makes the interfacial tension high, which leads to the formation of large emulsion droplets. The process of agglomeration into droplets results in the decrease in the number of emulsion droplets and the increase in the average diameter of emulsion droplets.

As the size of the emulsion droplets gradually increases, the stability of the oil−water interface is weakened, which eventually leads to the breakdown of the emulsion droplets and the reseparation of the oil−water phases.[30] The emulsion droplets rupture occurred in a large area with a low FMP concentration. After the oil phase aggregates again, an oil-rich region is formed. In the oil-rich region, the oil phase becomes continuous, which increases the mobility of the oil phase.[31]

In addition, several different microscopic phenomena may occur simultaneously in the same area of the reservoir, which depends on the concentration of the FMP solution and the pore-throat characteristics in the area of the reservoir.

3.4. Microscopic Explanations of Macroscopic Phenomena. According to the macroscopic image and production dynamic curve, it can be seen that FMP solution flooding can significantly enhance heavy oil recovery. On the one hand, FMP solution flooding can enhance the displacement efficiency of the remaining oil, and on the other hand, the FMP solution can also expand the areal sweep efficiency.

During the process of membrane oil removal, the adhesion membrane oil is removed in the SSZ. In the process of gradual emulsion, the removed membrane oil formed emulsion droplets, which had better mobility in the porous media. As shown in Figure 12b,c, the process of membrane oil removal and gradual emulsion could make the percolation channels from dark to bright in the SSZ, which means that the two processes play an important role in improving the displacement efficiency of the reservoir.[32,33]

When the concentration of FMP solution is low in the reservoir, the processes of flocculation into droplet groups and agglomeration into droplets are easy to occur, which leads to the generation of large emulsion droplets.[34−36] Large emulsion droplets are stuck in the pore-throat of the SSZ, which causes the blockage zone to appear. As shown in Figure 5e, the blockage zone causes the formation of the ESZ in the macroscopic image. Meanwhile, it can be seen from Figure 12b,c that oil spots subsided in the SSZ. The disappearance of oil spots in the SSZ and the appearance of the ESZ indicate that the FMP solution entered the unswept region and enlarged the sweep area of the reservoir.

4. CONCLUSIONS

(1) Compared with water flooding, the areal sweep coefficient of FMP flooding increases from 0.56 to 0.90 and the oil recovery is increases from 18 to 34%, which indicates that FMP enhanced the performance of the heavy oil reservoir.

(2) The appearance and disappearance processes of emulsion droplets become a process that is beneficial for improving oil recovery under the influence of the FMP concentration and the pore-throat structure. It is of great significance to observe heavy oil emulsification during the displacement process by the visual filling model.

(3) FMP molecules can affect the interfacial properties of oil, water, and rock, which can promote the membrane oil removal and gradual emulsification to enhance the wishing oil efficiency. FMP molecules affect the oil−water interfacial stability, which can promote flocculation into droplet groups and agglomerate into droplets to expand the sweep region.

AUTHOR INFORMATION

Corresponding Author

Qing Wang − *School of Petroleum Engineering, China University of Petroleum, Beijing 102249, China*; Email: wq2012@cup.edu.cn

Authors

Yu Li − *School of Petroleum Engineering, China University of Petroleum, Beijing 102249, China*

https://doi.org/10.1021/acsomega.1c03366
ACS Omega 2021, 6, 24663−24671

Huiqing Liu − *School of Petroleum Engineering, China University of Petroleum, Beijing 102249, China;* orcid.org/0000-0002-1149-4929

Xiaohu Dong − *School of Petroleum Engineering, China University of Petroleum, Beijing 102249, China;* orcid.org/0000-0002-4754-6188

Xin Chen − *Research Institute of Unconventional Petroleum Science and Technology, China University of Petroleum, Beijing 102249, China*

Complete contact information is available at: https://pubs.acs.org/10.1021/acsomega.1c03366

Notes

The authors declare no competing financial interest.

■ ACKNOWLEDGMENTS

The research work is supported by the National Natural Science Foundation of China (no. U20B6003) and the Science Foundation of China University of Petroleum, Beijing (no. 2462020YXZZ032).

■ NOMENCLATURE

FMP, name of the novel polymer viscosity reducer; AM, fragment of acrylamide; AA, fragment of sodium acrylate; PB, fragment of 4-phenyl-1-butene; AMPS, fragment of acrylamide-2-methyl propyl sulfonic acid; R_o, viscosity reduction ratio (%); μ_i, apparent viscosity of the oil sample (mPa·s); μ_r, apparent viscosity of the oil sample mixed with FMP solution (mPa·s); SSZ, strong seepage zone; ESZ, extended seepage zone; S_c, areal sweep coefficient, fraction; A_S, sweep area (cm^2); A, visual area of the simulated reservoir (cm^2)

■ REFERENCES

(1) Yang, Z.; Ma, G.; Hu, Z.; Zhai, W. Characterization of ternary compound viscosity reducer system on viscosity of viscous crude oil. *Pet. Sci. Technol.* **2017**, *35*, 1910−1916.

(2) Bryan, J.; Kantzas, A. Potential for Alkali-Surfactant Flooding in Heavy Oil Reservoirs Through Oil-in-Water Emulsification. *J. Can. Pet. Technol.* **2009**, *48*, 37−46.

(3) Ali, S. M. F.; Meldau, R. F. Current Steamflood Field Experience. *SPE Annual Fall Technical Conference and Exhibition*; OnePetro 1978.

(4) Meldau, R. F.; Doscher, T. M.; Ali, S. M. F.; Chu, C.; Holm, L. W.; Orr, F. M., Jr.; Gogarty, W. B.; Hause, W. R.; Reed, R. L.; Mayer, E. H. Experts Assess Status and Outlook for Thermal, Chemical, and CO2 Miscible Flooding Processes. *J. Pet. Technol.* **1983**, *35*, 1279−1291.

(5) Zhang, F.; Ma, D.; Tian, M.; Luo, W.; Zhu, Y.; Luo, Y.; Liu, W. Study on a Novel Viscosity Reducer for High Viscosity and Low Permeability Reservoirs. *SPE Middle East Oil & Gas Show and Conference*; OnePetro 2017.

(6) Mohammed, M.; Babadagli, T. New insights into the interfacial phenomena occurring between hydrocarbon solvent and heavy oil. *J. Pet. Sci. Eng.* **2021**, *196*, 108022.

(7) Lee, J.; Huang, J.; Babadagli, T. Visual Support for Heavy-Oil Emulsification and its Stability for Cold-Production using Chemical and Nano-Particles. *SPE Annual Technical Conference and Exhibition*; OnePetro 2019.

(8) Guo, Y.; Liu, W. D.; Xiu, J. L.; Sun, L. H.; Luo, L. T.; Xu, K. A Study on the Effects of Interfacial Tension on Emulsion Formation for SP Binary Flooding. *Pet. Sci. Technol* **2015**, *33*, 1479−1484.

(9) Geng, J.; Fan, H.; Zhao, Y.; Kang, W. A correlation between interfacial tension, emulsifying ability and oil displacement efficiency of ASP system for Daqing crude oil. *Pet. Sci. Technol.* **2018**, *36*, 2151−2156.

(10) Liu, Y.; Iglauer, S.; Cai, J.; Amooie, M. A.; Qin, C. Local instabilities during capillary-dominated immiscible displacement in porous media. *Capillarity* **2019**, *2*, 1−7.

(11) Voroniak, A.; Bryan, J. L.; Hejazi, H.; Kantzas, A. Two-Dimensional Visualization of Heavy Oil Displacement Mechanism During Chemical Flooding. *SPE Annual Technical Conference and Exhibition*; OnePetro 2016.

(12) Huang, K.; Zhu, W.; Sun, L.; Wang, Q.; Liu, Q. Experimental study on gas EOR for heavy oil in glutenite reservoirs after water flooding. *J. Pet. Sci. Eng.* **2019**, *181*, 106130.

(13) Yu, F.; Jiang, H.; Xu, F.; Zhen, F.; Wang, J.; Cheng, B.; Su, H.; Li, J. A multi-scale experimental study of hydrophobically-modified polyacrylamide flood and surfactant-polymer flood on enhanced heavy oil recovery. *J. Pet. Sci. Eng.* **2019**, *182*, 106258.

(14) Shan, L.; Lu, X.-L.; Shan, R.-Q.; Zhu, Y.-T.; Liu, J. Profile control and oil displacement by gel EOR for heavy oil reservoirs. *Spec. Oil Gas Reservoirs* **2010**, *17*, 72−75.

(15) Roosta, A.; Escrochi, M.; Varzandeh, F.; Khatibi, J.; Ayatollahi, S.; Shafiei, M. Investigating the Mechanism of Thermally Induced Wettability Alteration. *SPE Middle East Oil and Gas Show and Conference*; OnePetro 2009.

(16) Herbas, J. G. G.; Wegner, J.; Hincapie, R. E. E.; Födisch, H.; Ganzer, L.; Castillo, J. A. D.; Mugizi, H. M. Comprehensive Micromodel Study to Evaluate Polymer EOR in Unconsolidated Sand Reservoirs; *SPE Middle East Oil & Gas Show and Conference*; OnePetro 2015.

(17) Zhang, Y.; Khorshidian, H.; Mohammadi, M.; Sanati-Nezhad, A.; Hejazi, S. H. Functionalized multiscale visual models to unravel flow and transport physics in porous structures. *Water Res.* **2020**, *175*, 115676.

(18) Pratama, R. A.; Babadagli, T. Tertiary-Recovery Improvement of Steam Injection Using Chemical Additives: Pore Scale Understanding of Challenges and Solutions Through Visual Experiments. *SPE J.* **2021**, 1552.

(19) Lyu, X.; Liu, H.; Pang, Z.; Sun, Z. Visualized study of thermochemistry assisted steam flooding to improve oil recovery in heavy oil reservoir with glass micromodels. *Fuel* **2018**, *218*, 118−126.

(20) Meriem-Benziane, M.; Abdul-Wahab, S. A.; Benaicha, M.; Belhadri, M. Investigating the rheological properties of light crude oil and the characteristics of its emulsions in order to improve pipeline flow. *Fuel* **2012**, *95*, 97−107.

(21) Akiyama, E.; Kashimoto, A.; Hotta, H.; Kitsuki, T. Mechanism of oil-in-water emulsification using a water-soluble amphiphilic polymer and lipophilic surfactant. *J. Colloid Interface Sci.* **2006**, *300*, 141−148.

(22) Orrego-Ruiz, J. A.; Medina-Sandoval, C. F.; Hinds, C. C.; Villar-Garcia, Á.; Rojas-Ruiz, F. A. FT-ICR MS determination of the role of naphthenic acids on the stabilization of alkali/surfactant/polymer emulsified effluents: A field study. *J. Pet. Sci. Eng.* **2019**, *179*, 192−198.

(23) Sun, Z.; Kang, X.; Lu, X.; Li, Q.; Wu, X. The influence of oil property on interfacial tension. *Pet. Sci. Technol.* **2019**, *37*, 2315−2321.

(24) Li, B.; Tao, L.; Zhang, N.; Wang, K.; Li, Z. The influence of surfactants on the flow characterization of heavy oil. *Pet. Sci. Technol.* **2019**, *37*, 155−162.

(25) Wang, Y.; Liu, H.; Zhang, Q.; Chen, Z.; Wang, J.; Dong, X.; Chen, F. Pore-scale experimental study on EOR mechanisms of combining thermal and chemical flooding in heavy oil reservoirs. *J. Pet. Sci. Eng.* **2020**, *185*, 106649.

(26) Wang, Y.; Liu, H.; Wang, J.; Dong, X.; Chen, F. Formulation development and visualized investigation of temperature-resistant and salt-tolerant surfactant-polymer flooding to enhance oil recovery. *J. Pet. Sci. Eng.* **2019**, *174*, 584−598.

(27) Luo, X.; Huang, X.; Yan, H.; Yang, D.; Zhang, P.; He, L. An experimental study on the coalescence behavior of oil droplet in ASP solution. *Sep. Purif. Technol.* **2018**, *203*, 152−158.

(28) Khayati, H.; Moslemizadeh, A.; Shahbazi, K.; Moraveji, M. K.; Riazi, S. H. An experimental investigation on the use of saponin as a non-ionic surfactant for chemical enhanced oil recovery (EOR) in sandstone and carbonate oil reservoirs: IFT, wettability alteration, and oil recovery. *Chem. Eng. Res. Des.* **2020**, *160*, 417−425.

(29) Zhao, G.; Dai, C.; Wen, D.; Fang, J. Stability mechanism of a novel three-Phase foam by adding dispersed particle gel. *Colloid Surf. A* **2016**, *497*, 214−224.
(30) Zhao, X.; Feng, Y.; Liao, G.; Liu, W. Visualizing in-situ emulsification in porous media during surfactant flooding: A micro-fluidic study. *J. Colloid Interface Sci.* **2020**, *578*, 629−640.
(31) Erk, K. A.; Martin, J. D.; Schwalbe, J. T.; Phelan, F. R., Jr.; Hudson, S. D. Shear and dilational interfacial rheology of surfactant-stabilized droplets. *J. Colloid Interface Sci* **2012**, *377*, 442−449.
(32) Yu, L.; Dong, M.; Ding, B.; Yuan, Y. Experimental study on the effect of interfacial tension on the conformance control of oil-in-water emulsions in heterogeneous oil sands reservoirs. *Chem. Eng. Sci.* **2018**, *189*, 165−178.
(33) Yang, C. Experimental study on the viscosity reduction of heavy oil by using of a new type of micro-emulsion. *Pet. Sci. Technol.* **2019**, *37*, 1394−1399.
(34) Wei, B.; Hou, J.; Sukop, M. C.; Du, Q.; Wang, H. Flow behaviors of emulsions in constricted capillaries: A lattice Boltzmann simulation study. *Chem. Eng. Sci.* **2020**, *227*, 115925.
(35) Arab, D.; Kantzas, A.; Bryant, S. L. Water flooding of oil reservoirs: Effect of oil viscosity and injection velocity on the interplay between capillary and viscous forces. *J. Pet. Sci. Eng.* **2020**, *186*, 106691.
(36) Dong, X.; Liu, H.; Chen, Z.; Wu, K.; Lu, N.; Zhang, Q. Enhanced oil recovery techniques for heavy oil and oilsands reservoirs after steam injection. *Appl. Energy* **2019**, *239*, 1190−1211.

https://doi.org/10.1021/acsomega.1c03366
ACS Omega 2021, 6, 24663−24671